Published in final edited form as:
J Phys Chem B. 2012 March 15; 116(10): 3467–3475. doi:10.1021/jp300392a.

Photoinduced Electron Transfer in Folic Acid Investigated by Ultrafast Infrared Spectroscopy

Guifeng Li, **Donny Magana**, and **R. Brian Dyer***
Department of Chemistry, Emory University, Atlanta, Georgia, 30322, United States

Abstract

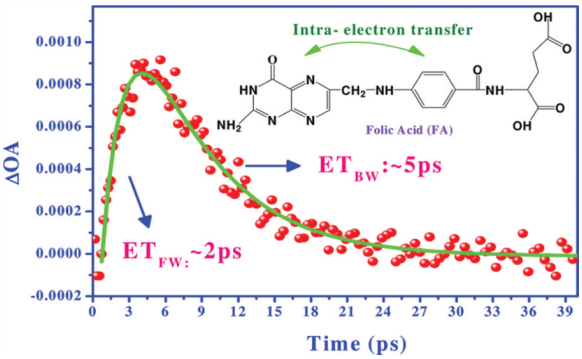

Conformational control of excited-state intramolecular electron transfer (ET) in folic acid (FA) has been investigated using femtosecond time-resolved infrared (TRIR) spectroscopy. Ultrafast excited-state ET between the pterin and the 4-aminobenzoyl subunits of FA is observed for the anionic form (at pH 10.0). An ET lifetime of 2.5 ps is estimated from Marcus theory for FA in the "U" conformation, in close agreement with the observed lifetime of 2.0 ps. Return to the ground state through the reverse ET reaction happens almost as rapidly, within 5 ps, resulting in rapid quenching of the singlet excited state. In mixed water:dimethyl sulfoxide solvent, ET becomes more unfavorable as FA adopts a more open conformation, thereby increasing the effective donor–acceptor distance and reducing the coupling energy. In contrast, no ET is observed for the cationic form of FA at low pH (6.0). In this case, the initial singlet excited state is localized on the pterin moiety of FA, and the excited-state charge distribution evolves with time. The charge redistribution in the pterin that occurs with intersystem crossing to the triplet state is characterized by changes in the transient IR spectrum. The excited-state lifetime is much longer in the absence of an ET quenching pathway. These results provide new insight into the mechanism of photodegradation and toxicity of FA. Ultrafast intramolecular ET in closed conformations of FA rapidly quenches the excited state and prevents efficient triplet state formation. Thus, conformations of FA that allow ultrafast intra-ET and rapid quenching of the singlet excited state play a key role in inhibiting pathological pathways following photoexcitation of FA.

***Corresponding Author**, Phone: +1-404-727-6637; briandyer@emory.edu.

ASSOCIATED CONTENT

Supporting Information

Supporting Information material contains supporting figures as indicated in the text. This material is available free of charge via the Internet at http://pubs.acs.org.

The authors declare no competing financial interest.

INTRODUCTION

Folic acid (FA), water-soluble vitamin B_9, is required for normal tissue growth and development,[1,2] and plays an important role in the metabolism of amino acids and biosynthesis of DNA and RNA.[1–3] FA may also have potential applications in cancer prevention[3–5] through its free-radical scavenging and antioxidant activity.[6] However, FA has a Jekyll and Hyde-like nature because excess intake may increase the risk of skin cancer caused by ultraviolet (UV) light exposure, due to FA-related DNA cleavage.[7] The mechanism of FA related to DNA damage appears to be electron transfer (ET) between consecutive G residues and photoexcited pterine-6-carboxylic acid (PCA), which is a product of UV photo-degradation of FA.[7,8]

Despite the biological importance of the photochemistry and photophysics of FA, they are not yet fully understood. Recent studies have mainly focused on the photodegradation of FA or pterins observed by UV absorbance[9,10] and fluorescence.[10–12] In addition, computational methods have been applied to the understanding of its photochemical and photophysical processes.[13–16] Most studies of FA photochemistry suggest that photoinduced ET between the components of FA may play an important role in its photodegradation.[7,11,13] However, such a mechanism is not completely supported by the available evidence, which is mostly indirect, including theoretical calculations and experimental measurements such as fluorescence quenching. Furthermore, the role of FA conformation in the ET dynamics is not understood. Therefore, the ET mechanism in FA continues to be controversial and in need of clarification. Two different models have been proposed to explain the photoinduced ET reactions of FA. One model is intramolecular electron transfer (intra-ET) between the pterin ring and the 4-aminobenzoyl ring of FA. This model is supported indirectly by differences in the fluorescence spectra of FA and its components, PCA and *p*-aminobenzoyl-L-glutamic acid (PABGA).[17] Another model is intermolecular electron transfer (inter-ET), due to vertical stacking of the hydrophilic or hydrophobic ring structures, which was postulated on the basis of concentration-dependent measurements.[18]

It should be possible to determine which of these mechanisms best describes the earliest ET processes in FA using ultrafast spectroscopy to probe the events that follow electronic excitation. A few studies have been carried out to probe radical formation in FA caused by reaction with free radicals such as •OH, using pulse radiolysis techniques.[6,19–21] Unfortunately, the time scale of such measurements is microseconds or slower, preventing direct observation of the initial ET reaction. Another critical issue is probing the excited-state dynamics with sufficient structural specificity to definitively assign the ET process.

We have employed femtosecond time-resolved infrared spectroscopy (TRIR) in order to capture the fast ET processes in FA. Previous work has demonstrated that TRIR spectroscopy is a powerful technique for following ET dynamics in complex molecular structures.[22–28] In comparison with ultrafast electronic spectroscopy in the UV–visible (UV/vis) range, infrared spectroscopy is more specific for characterization of radical formation in FA. In this work, we report the first ultrafast TRIR spectra and dynamics of FA and PCA. Two fast processes following photoexcitation of FA (2 and 5 ps, respectively) are observed for FA in high-pH solution (10.0). These processes are assigned to forward and backward ET between the 4-aminobenzoyl ring and the pterin ring, based on the unique IR signatures of the respective structures (obtained from comparison to the IR spectra of the component PCA and PABGA structures). This interpretation is further supported by a Marcus analysis of the ET rate. A Gibbs free energy calculation for the ET reactions predicts that electron exchange is favorable in the excited state, providing an efficient mechanism for quenching of the excited state. The intra-ET model is further supported by concentration and solvent-dependent measurements in high-pH solution. By contrast, FA does not exhibit excited-state

ET in low-pH solution (6.0). Instead, the TRIR spectra indicate a long-lived singlet state localized on the PCA that ultimately converts to a triplet state via intersystem crossing (ISC) with a concomitant redistribution of the charge on the pterin rings. We rationalize these results in terms of the changes in the conformation of FA that control the ET transfer rate by changing the donor–acceptor distance and the coupling energy.

EXPERIMENTAL SECTION

Chemicals

FA ($C_{19}H_{19}N_7O_6$, ≥97%), PCA ($C_7H_5N_5O_3$, ≥98.0% HPLC), deuterium oxide (D_2O, 99.9 atom %D), potassium deuteroxide (KOD, 40% wt % solution in D_2O 98+ atom %D), and deuterium chloride solution (35 wt % in D_2O, 99 atom % D) were received from Sigma-Aldrich and used without further purification. PABGA (MP Biomedical) and dimethyl sulfoxide (DMSO, 99.9%, EMD) were used as received. The chemical structures of FA, PCA, and PABGA are shown in Figure 1.

Fifty millimolar phosphate buffer solution (pH = 7.0) was prepared from potassium phosphate monobasic (KH_2PO_4, ACS reagent) and potassium phosphate dibasic (K_2HPO_4, ACS reagent) in a 1:1 ratio in D_2O. FA was dissolved into 1–2 mL of buffer solution by adding KOD, and an additional 6 mL of buffer solution was transferred into the 1–2 mL FA stock solution to produce final concentrations of 5, 10, 20, 60, and 80 mM FA. The uncorrected (for D_2O) pH value of the solution is adjusted to 10 and 6.0 using a pH meter (Fisher Scientific, Accumet AB15Basic) for the TRIR measurements. It has been established previously that the pterin ring of FA undergoes protonation of N(3) with a pK_a of ~8.3,[29] which generates basic and acidic forms accompanied by the keto–enolisomerization of the carbonyl. Also, the N(5) position in the pterin ring has a protonation transition with a pK_a of ~6.6.[29] These transitions are also summarized in Figure 2. In summary, FA is expected to exist in its cationic form at pH 6.0, its neutral form at pH 7.0, and its anionic form at pH 10.0.

For solvent-dependent TRIR measurements, FA was first dissolved into a 50 mM phosphate buffer solution (pH 7.0), then mixed with DMSO to obtain a 60 mM FA solution in DMSO/D_2O having 10:0, 8:2, 5:5, 2:8, and 0:10 (v/v) ratios. Concentration-dependent TRIR measurements of FA were carried out in 80, 60, 20, and 5 mM phosphate buffer solutions. The pK_a of FA was determined by pH-dependent UV and Fourier transform infrared (FTIR) measurements of 10 mM FA solutions. In the same way, the pK_a of PCA was determined by pH-dependent UV and FTIR measurements in 10 mM PCA solutions.

Femtosecond TRIR Measurements

Transient infrared absorption spectra are obtained using a femtosecond pump–probe technique. The TRIR system is described briefly as follows: 800 nm laser pulses (1 kHz repetition rate, 30 fs pulse width) are generated from a femtosecond Ti:sapphire regenerative amplifier (Legend Elite, Coherent) seeded by a femtosecond Ti:sapphire mode-locked oscillator (Mantis, Coherent). The 3.6 W output power from the Legend is split in a 1:1 ratio and sent into two OPA systems (OPerA Solo, Coherent) that are used to generate UV and IR laser beams, respectively. The excitation wavelength is 400 nm, directly generated by doubling the frequency of the 800 nm fundamental in a nonlinear β-barium borate (BBO) crystal. The 400 nm pump beam is delayed by a computer-controlled translation stage (Newmark System, Inc.). The IR laser beam generated by a difference frequency mixing the signal and idler beams from the OPA in a nonlinear crystal (AgGaS) is separated into probe and reference beams by a CaF_2 beamsplitter (50/50 ± 10% R/T, 2–8 μm, ISP Optics), then dispersed in an IR spectrograph and detected with a multichannel infrared focal plane array

(ImagIR, HgCdTe, 2–10 μm, 128 × 128, Santa Barbara Focalplane). An optical chopper (3501, New Focus Inc.) is used to modulate the excitation beam at 500 Hz frequency to obtain light-on and light-off single beam. IR spectra, from which the transient IR absorption signal is calculated as $\Delta A = -\log(I_{on}/I_{off})$. The relative polarization between the pump and probe beams is set at the magic angle (54.7°). The 10 mW, 400 nm pump beam is focused on the sample and overlaps with the IR probe beam, and the data acquisition is achieved using LabVIEW (National Instruments).

The sample solution is flowed through a demountable liquid flow cell with swagelok fittings (DSC-S25, Harrick Scientific Product Inc.) using a fluid metering RHSY lab pump (Scientific Support Inc.). The path length is 80 μm for all transient spectra reported here, which is set by a Teflon spacer between two polished circular CaF_2 windows (25 × 2 mm, Koch Crystal Finishing, Inc.).

FT-IR and UV/vis Measurements

FTIR and UV/vis spectra were obtained from aqueous solutions of FA, PCA, and PABGA using a DIR amalgamated sealed cell (McCarthy Scientific Co.) consisting of two polished rectangular CaF_2 windows (38.5 × 19.5 × 4 mm, Koch Crystal Finishing, Inc.) separated by a Teflon spacer (80 μm). Steady-state IR spectra were collected using a Varian 660 FTIR Spectrometer (1 cm^{-1} resolution, 256 scans), while steady-state UV/vis spectra were collected using a Lambda35 spectrophotometer (Perkin-Elmer).

RESULTS AND DISCUSSION

Spectral Characterization of the Ground States of FA, PCA, and PABGA

Figure 3A shows the ground-state IR spectra of FA, PABGA, and PCA at pH 9.6. The FA spectrum is well modeled as a linear combination of the spectra of the two structural subcomponents PCA and PABGA. Therefore the IR peaks due to each structural subcomponent of FA are easily assigned by comparison with the PCA and PABGA spectra. The peaks at 1593 and 1561 cm^{-1} in the FTIR spectrum of FA (Figure 3A) are from PABGA, attributed to the aromatic ring breathing mode (ν_{8a}) and ν_{COO-} (asymmetric stretch).[30] Above pH 8.3 (FA in its anionic form, as shown in Figure 2), a band appears around 1580 cm^{-1} that we assign to the $C_4{=}N_3$ stretching mode of the pterin ring by analogy to flavin. Flavin has a heterocyclic ring structure similar to that of pterin and exhibits a $C_{4a}{=}N_5$ stretching mode at 1578 cm^{-1}.[31] The FA peaks at 1542 and 1520 cm^{-1} (Figure 3A) are from the C═C stretches of the heterocyclic ring and heterocyclic ring breathing in PCA.[32] The peaks at 1608 (FA), 1610 (PABGA), and 1603 (PCA) cm^{-1} in Figure 3A are from the C–N stretch of the $–C(NH_2)$ group present in each of these structures.[30,33,34] By comparison with the UV spectra of PABGA and PCA in Figure 3B, the broad band around 365 nm in FA is assigned to the π−π* transition localized on the pterin ring in FA. The other peaks at 255 and 280 nm are also from π−π* transitions of the pterin ring,[14,35] while the shoulder at 290 nm is related to the π−π* transition localized on the 4-aminobenzoyl ring of PABGA.[35] The peak at 255 nm only appears at high pH (pH > pK_a = 8.3), due to deprotonation of N(3) in the anionic form of FA.[29]

Distinct differences are observed in the FTIR and UV absorbance when the pH is lowered from 9.6 (Figure 3C,D). At a pH lower than 8.3,[8,12] the N(3) position of the pterin ring becomes protonated, which induces a dramatic change in the –N(3)–C(4)– coordinate of the pterin ring structure (Figure 2), from –;N═C(−OH)– to –N(H)–C(═O)–. For the neutral form of FA (data not shown), the peak at 1672 cm^{-1} assigned to $C_4{=}O$ is broad, which suggests that this band may be involved in a resonance effect between N(3)H and $C_4{=}O$. A further decrease of the pH to 6.2 causes the N(5) position to become protonated (pK_a = 6.6;

Figure 2). A sharp peak at 1667 cm^{-1} dominates the pH 6.2 spectrum of FA, as shown in Figure 3C, and appears to be characteristic of the cationic form of the pterin structure.[29] If this band is due to the C_4═O stretch, it is much sharper and shifted to lower frequency compared to the anionic and neutral forms. A possible reason for these differences is the formation of a strong hydrogen bond between the pterin keto group and the nearby imine (C_4═O···H–N_5). This interpretation is not consistent with the IR spectra of guanine tetrad structures, however, in which hydrogen-bonding induces a shift of the carbonyl stretch to higher frequency.[36] The same effect has been observed for guanosine in acidic solution: the protonation of position 7 in 5′-guanosine monophosphate (5′-GMP) removes electron density from the pyrimidine ring. The subsequent decoupling of the C═O stretch from the solvent through weaker hydrogen bonding leads to a high frequency shift of this mode.[37] An alternative assignment for the sharp band in cationic FA is suggested by the IR spectrum of adenosine as shown in the Supporting Information (Figures S1 and S2). Neutral adenosine shows a broad band at 1625 cm^{-1}, while its acidic form exhibits a sharp and strong band at 1668 cm^{-1} due to protonation (pK_a = 3.5) of the heterocyclic ring. By analogy, protonation of the N(5) position of FA increases the double-bond nature of the C═N ring,[38] producing the sharp IR peak at 1667 cm^{-1} in Figure 3C due to the C═N_5 stretch. The shoulder at 1720 cm^{-1} is assigned to the COOH groups in PABGA, partially protonated as the pH approaches its pK_a value (4.8), which is confirmed by IR results for PABGA in low-pH solution. The UV spectra at pH 6.2 (Figure 3D) show no significant differences in comparison with pH 7, except for a slight peak intensity change around 365 nm.

(1). Excited States of FA, PCA, and PABGA—*TRIR Results for PCA and FA in Basic Solution.* Figure 4A compares the ground-state (GS) FTIR spectrum and TRIR spectrum (3 ps) of 40 mM PCA at pH 10. The broad negative peak around 1608 cm^{-1} is due to bleaching of the –C(NH_2)– stretch of the pterin ring. The IR transient monitored near the bleach maximum at 1608 cm^{-1} clearly consists of two components (τ_1 = 250 ± 20 ps and τ_2 > 1 ns), as shown in Figure 4B. We assign the short-lived component (250 ps) to ISC to form the triplet state of PCA, by comparison to the known fluorescence behavior of PCA.[12] The long-lived component corresponds to decay of the triplet state and perhaps some contribution of water heating.[39]

Figure 4C compares the GS FTIR spectrum with TRIR spectrum (3 ps) of 60 mM FA at pH 10. By analogy to PCA, the broad negative peak around 1608 cm^{-1} in the TRIR of Figure 4C arises from the –C(NH_2) stretch of the pterin ring, while the peak at 1593 cm^{-1} is from the aromatic ring of PABGA. The pump wavelength of 400 nm excites the pterin ring exclusively, since the 4-aminobenzoyl ring of the PABGA moiety does not absorb at this wavelength. If no further evolution of the system occurs on this time scale (such as ET), the TRIR spectra of FA and PCA excited at 400 nm should be identical. Comparison of the 3 ps TRIR spectra of PCA and FA (Figure 4A,C) reveals that they are not the same: FA exhibits a new peak near 1590 cm^{-1}, corresponding to the ν_{8a} mode of the 4-aminobenzoyl ring in PABGA. The bleach of this PABGA mode indicates a further evolution of the system following the local excitation of the pterin moiety, consistent with an ET process between the 4-aminobenzoyl ring of PABGA and the pterin ring of PCA. At first glance, a puzzling aspect of the TRIR spectrum of FA is the absence of any positive features corresponding to the ET (radical) state. This absence of any transient absorbance at pH 10 is a consequence of overlapping excited- and ground-state features, as we demonstrate with the pH-dependent measurements described below. The lifetimes of the transient IR features provide further support for an excited state ET. The 1608 cm^{-1} TRIR transients for PCA and FA following 400 nm excitation are compared in Figure 4D. The decay of the PCA singlet excited state has a lifetime of 250 ± 20 ps, due to ISC to the triplet state as discussed previously, while the decay of the analogous singlet excited state in FA is 2 orders of magnitude faster. Fitting the TRIR transient for FA (Figure 4D) to an exponential function yields a fast, dominant

component (5.9 ps) and a minor component with a much longer lifetime (significantly longer than the time scale of the measurement). We assign the fast component to intramolecular ET between the 4-aminobenzoyl ring and the pterin ring in FA. Thus, for FA the excited state localized on the pterin ring is rapidly quenched by intra-ET, in contrast to PCA where no intra-ET is possible. The long component is likely due to heating of the solvent, either through the ET relaxation pathway, or through radiationless decay of the FA excited state (internal conversion, IC) followed by vibrational relaxation and heat flow from FA to D_2O. D_2O has a broad, temperature-dependent absorbance in this region. Vibrational relaxation of the electronic excitation energy and thermalization with water can occur within a few picoseconds, and the water heating results in a bleach of the D_2O IR spectrum in this region that persists for about 1 ms, the time scale for cooling to the surroundings.[40] Similar transient IR signatures have been observed for IC and D_2O heating in related molecules such as malachite green.[41]

The TRIR spectrum should reflect the production of the radical species in the charge separated state (D^+A^-) following excited-state ET. Figure 5A shows the TRIR spectra of 60 mM FA (pH 9.6) from 1 to 20 ps following excitation with 400 nm light. The TRIR spectra of FA lack the peak at 1520 cm^{-1} assigned to a ring stretching mode of PCA (compare the ground-state spectrum of PCA in Figure 3A). The 1520 cm^{-1} peak is also absent in the ground-state IR spectrum of FA at low pH (6.0) as shown in Figure, 3C. Thus, protonation of N(3) causes the 1520 cm^{-1} peak to disappear, meaning that this mode is associated with the pterin ring that contains N(3) and the carbonyl group (the left ring of the structure as drawn in Figure 2). We conclude that the absence of the peak at 1520 cm^{-1} in the TRIR spectrum suggests the formation of an excited-state mainly localized on the right ring of the pterin. However, the appearance of a band at 1608 cm^{-1} in the TRIR spectrum, assigned to the amine substituent, suggests that the excitation is not completely localized on the right ring.

The time-dependent evolution of the TRIR spectrum in Figure 5A is wavelength dependent, which is particularly evident at 1608 and 1585 cm^{-1} (positions marked by dashed arrows), frequencies corresponding to pterin and 4-aminobenzoyl IR bands, respectively. The temporal profiles at 1608 cm^{-1} and 1585 cm^{-1} are compared in Figure 5B. Clear differences exist between the two transients, consistent with their assignment to separate processes. The bleach of the pterin absorbance at 1608 cm^{-1} occurs with an instrument limited rise of about 200 fs and clearly corresponds to formation of the localized pterin singlet excited state by the initial excitation, whereas the transient monitored at the 4-aminobenzoyl absorbance at 1585 cm^{-1} probes intra-ET. Overlap of these features obscures the actual kinetics of the intra-ET. We obtained the pure time profile for the intra-ET process by subtracting the 1608 cm^{-1} transient from the 1585 cm^{-1} transient, revealing the rise and decay of the radical signature (Figure 5B). By using the same method throughout this spectral region, we find that the transient absorbance of the charge-separated state has a peak around 1577 cm^{-1}. A weak transient absorbance (100–200 μOD) is observed directly at 1577 cm^{-1} from 60 mM FA, without subtraction of the ground state bleach, having the same time profile as shown in Figure 5B. The 1577 cm^{-1} feature of the charge-separated state is likely a PABGA radical mode, based on the strong bands observed in this region for the PABGA radical ground state. The raw transient at 1577 cm^{-1} is weak and contains a water heating background, making it difficult to fit the temporal profile. The subtraction method used to generate the decay profile at 1585 cm^{-1} (Figure 5B) removes the water heating background, making it possible to extract the rise and decay of the radical signal. The fit of this transient to an exponential rise and decay (Figure 5C) yields a lifetime of 2.0 ps for the forward ET from pterin to 4-aminobenzoyl, while the backward ET from 4-aminobenzoyl to pterin (recovery of the ground state) has a lifetime of 5.0 ps. The transient absorbance at 1630 cm^{-1} due to the pterin can also be used to follow recovery of the pterin ground state. Figure 5D shows

that the transient at 1630 cm^{-1} has a lifetime of 4.4 ps, meaning that recovery of the ground state occurs with the same lifetime as the backward ET (5.0 ps).

Additional insight into the excited-state dynamics of FA can be obtained by considering the driving force for ET in the singlet state. Previously, a free energy analysis of nanosecond ET for the triplet state of FA in DMSO was performed using the Rehm–Weller equation.[20] That calculation predicts a free energy change of −0.75 eV for ET from the 4-aminobenzoyl donor (E_{ox} = +0.88) to the triplet state of the pterin acceptor (E_{red} = −0.77) in DMSO. The ultrafast processes probed in our measurements correspond to the dynamics of the singlet state, therefore we evaluated the energetics of ET in this state using the Rehm–Weller equation. The redox potentials of PCA in the singlet excited state may be estimated using the ground-state redox potentials[42,43]

$$E^*_{ox} = E_{ox} - E_{00} \quad (1)$$

$$E^*_{red} = E_{red} + E_{00} \quad (2)$$

where E_{ox} * and E_{red}* are the oxidation and reduction potentials of PCA in the excited state, while E_{ox} and E_{red} are the oxidation and reduction potentials of PCA in the ground state. E_{00} is the energy difference between the ground state and the first excited (singlet) state obtained from the intersection of the normalized absorption and fluorescence emission spectra, which for PCA is 3.06 eV. The oxidation (E_{ox}, PCA) and reduction (E_{red}, PCA) potentials of PCA in the ground state are +1.31 and −0.86 V, respectively. Thus, the excited state redox potentials are given by

$$E^*_{ox,PCA} = 1.31 - 3.06 = -1.75 \text{ V} \quad (3)$$

$$E^*_{red,PCA} = -0.86 + 3.06 = 2.20 \text{ V} \quad (4)$$

The Gibbs free energy change of ET from 4-aminobenzoyl to the singlet excited state of the pterin of FA can be evaluated using the excited-state redox potentials of PCA and the ground-state redox potential of PABGA in the Rehm–Weller equation. Therefore, if PCA is oxidized by PABGA, the change in Gibbs free energy is given by[43]

$$\Delta G_{PABGA-PCA} = E_{ox,PABGA} - E^*_{red,PCA} + \Delta G_0 \quad (5)$$

where ΔG_0 is the coulomb term (the solvation energy of the ion pair D^+A^- formed in the ET reaction). This term approaches zero for strongly polar solvents such as water. Neglecting ΔG_0 and using the ground-state oxidation potential of PABGA ($E_{ox,PABGA}$ = 0.93 V), $\Delta G_{PABGA\text{-}PCA}$ = 0.93–2.2 = −1.27 eV. Conversely, if PCA is reduced by PABGA, the Gibbs free energy change is given by $\Delta G_{PCA\text{-}PABGA}$ = −1.75 – (−0.57) = −1.18 eV.

Since $\Delta G_{PABGA\text{-}PCA}$ (−1.27 eV) and $\Delta G_{PCA\text{-}PABGA}$ (−1.18 eV) are very close in energy to one another, and both are spontaneous for ET, both ET processes are possible when PCA is excited by a 400 nm photon. Furthermore, each one-electron process may be followed by a second ET that carries the system back to the ground state. If the excited state is rapidly quenched by such an electron exchange process, it would be difficult to observe the radical formed by the single ET process. Such a mechanism may explain in part why it is difficult to observe any new positive absorbances in the TRIR spectra due to radical formation (along with the problem of overlapping GS and ES contributions), because the charge separated

state is short-lived. Charge recombination within the two possible radical states (PCA^{-}–$PABGA^{+}$ and PCA^{+}–$PABGA^{-}$) is complete within ps.

(2). TRIR Results for FA in Acidic Solution—The electrochemical behavior of PABGA strongly depends on the pH of the solution due to its amphoteric nature.[44] With increasing pH, the oxidation potential of PABGA decreases.[44] Likewise, the redox behavior of pterin is sensitive to the pH of the solution, although its pH dependence is different from that of PABGA.[45] Thus the redox potentials of both the ET donor and acceptor can be tuned to a different extent by changing the pH of the solution. If the relative driving force for the forward and reverse ET reactions is altered by the pH, it may be possible to increase the lifetime of the radical intermediate, making it easier to detect. Therefore, we carried out pH-dependent measurements to probe its effect on the ET dynamics in the excited state. What we found was perhaps even more interesting: lowering the pH completely inhibits the ET reaction, producing only a localized excitation on the pterin. We show below that the initial singlet excited state undergoes ISC to the triplet state, which has a very different charge distribution on the pterin moiety, making it possible to clearly distinguish this transition.

Figure 6A compares the FTIR and TRIR (2 ps) spectra of 5 mM FA at pH 5.8. The low-pH TRIR spectrum is remarkably different compared to the high-pH TRIR spectrum (Figure 5A). There are two bleach features at 1610 and 1680 cm^{-1}, which by comparison to the GS FTIR spectrum of FA (Figure 6A) and the assignments detailed above, are due to –N-(NH_2)– and carbonyl stretching modes, respectively. Both of these groups are part of the left ring of the pterin moiety. None of the GS features of the 4-aminobenzoyl are observed as bleaches, and no new absorbances attributable to the 4-aminobenzoyl are observed in the TRIR spectrum at pH 5.8, meaning that this part of the structure is not involved in the initial excitation or subsequent dynamics. We conclude that excited state ET does not occur in FA at low pH. The strong transient absorbance that appears at 1587 cm^{-1} is attributed to the pterin. Despite the localization of the initial excitation on the pterin moiety, not all of the GS features attributed to it appear as bleaches in the TRIR spectrum. Most prominently, the sharp band at 1667 cm^{-1} is absent in the TRIR spectrum. As noted above, this band is unique to the cationic form of FA and is due to the C═N stretch of the right ring of the pterin (lacking the carbonyl) that appears upon protonation of N(5). The absence of this band, and the dominant contribution of the –N(NH_2)– and carbonyl stretching modes in the TRIR spectrum suggests that the excited-state charge is localized on the left ring of the pterin.

The evolution of the pH 5.8 TRIR spectrum, shown in Figure 6B, indicates that there are multiple processes following 400 nm excitation. The initial excitation produces a bleach of the broad band at 1680 cm^{-1}, attributed to the pterin carbonyl stretch, as indicated by the dashed line in Figure 6B. This bleach relaxes with a lifetime of about 220 ps, accompanied by decay of the excited-state absorbance at 1587 and 1549 cm^{-1}. After 400 ps, the band at 1680 cm^{-1} has disappeared, while a weak bleach appears at 1667 cm^{-1} as indicated by the arrow in Figure 6B. This feature is due to the sharp band produced by protonation of N(5) that is assigned to the C═N stretch of the ring containing N(5). The intensity of the bleach at 1667 cm^{-1} increases as the broad bleach at 1680 cm^{-1} decreases. This transition between the 1680 and 1667 cm^{-1} bleaches indicates that following the initial absorbance, the excitation remains localized on the pterin moiety, but that the charge distribution between the two rings of the pterin evolves with time. The IR transients monitored at 1587, 1610, 1667, and 1680 cm^{-1} are compared in Figure 6C. All of these transients exhibit a fast decay (7 ps), which at first glance might seem to be consistent with the reverse ET rate observed at high pH. But none of the other indicators of ET are observed, particularly the IR features due to the reduction of the 4-aminobenzoyl structure. This 7 ps decay also shows a strong concentration dependence as shown below, and thus we assign it to the presence of a small fraction of FA dimers having a stacked geometry of the pterin rings that results in rapid

quenching of the excited state. In addition to the fast phase, slower relaxations are observed at most of the probe frequencies, with lifetimes of 220 ps and 2 ns. We assign the slow relaxation (220 ps) to ISC from the singlet to the triplet state of pterin, while the 2 ns process represents the return to the ground state. The 220 ps rise time is also consistent with the time scale observed for the reorganization of the excited-state charge distribution sensed by the relaxation of the carbonyl bleach at 1680 cm^{-1} and the growth of the C═N bleach at 1667 cm^{-1}. We conclude that the singlet and triplet excited states of pterin have very different charge distributions. In support of this interpretation, we note that the pH-dependent fluorescence quenching of pyrene by nucleic bases has been attributed to a charge transfer process that is mediated by pH.[46]

Why is the ET reaction not observed at low pH? A clue is provided by the changes in the UV–vis absorbance spectra (Figure 3B,D) induced by lowering the pH. The pH-dependent spectra clearly show a shift in energy of the lowest energy band near 365 nm with pH (Figure S3). This band is assigned to a $\pi-\pi^*$ transition localized on the pterin ring in FA. The shift is to higher energy with decreasing pH, as expected for conversion to the open form of FA, which results in a diminished interaction between the π systems of the pterin and 4-aminobenzoyl rings. Thus it is possible that FA adopts a more open conformation at low pH (6.0), which slows the ET reaction. It is also possible that the increased oxidation potential of the PABGA at low pH contributes to the slower ET rate. The combined effect of these changes is that ISC to the triplet state becomes the dominant process at low pH. Further support for this conclusion is provided by the fluorescence quantum yield of cationic FA, which is greater than that for the neutral and anionic forms of FA.[12] Since the excited state is rapidly quenched by ET for the anionic form but not for the cationic form, a higher quantum yield of ISC and triplet emission is observed for the latter case. Finally, our interpretation is consistent with previous investigations by Penzkofer of the fluorescence quenching behavior of FA as a function of solution conditions.[11] Different fluorescence quenching mechanisms were proposed for the different ionic forms: photophysical nonradiative relaxation for cationic FA, and photoinduced intramolecular ET for neutral and anionic FA.

(3). Dimerization of FA in Acidic and Basic Solution—The concentration-dependent dimerization of FA in basic and neutral solutions has been investigated by NMR spectroscopy.[47] This study found that the critical concentration for dimerization is different for the basic (340 mM) and neutral (19.4 mM) forms of FA.[47] In order to understand the differences in the photophysics and photochemistry between monomer and dimer, we carried out concentration-dependent measurements over the range of 5–60 mM FA. The concentration-dependent TRIR transients at 1610 cm^{-1} are compared in Figure 7A (pH 6.0) and B (pH 10.0). A strong concentration dependence is observed in pH 6.0 solution, with a fast decay (13 ps) observed at 20 and 60 mM, a slow decay observed at 5 mM, and both components observed for the intermediate case (10 mM). The break in behavior occurs exactly where the transition between monomer and dimer is observed in the NMR experiments. Thus we conclude that the short lifetime is associated with dimer formation, due to ring stacking. As a control experiment, we investigated similar dimer formation between PCA and tryptophan in aqueous solution. When tryptophan is introduced into PCA solution in a 1:1 ratio, the TRIR spectrum of PCA shows a fast relaxation of 5.6 ps, compared to the several hundred picosecond relaxation observed for PCA alone. Clearly the formation of a dimer with a stacked ring–ring interaction greatly shortens the lifetime of the pterin singlet excited state.

In high-pH solution (pH 10.0), FA is present as a monomer in the concentration range of 5–60 mM, since the critical concentration for dimer formation is 340 mM based on the NMR results. As expected, we observe no dependence of the IR transients on concentration in this

range, as shown in Figure 7B. The fast (7 ps) decay observed in this case is due to ET to the 4-aminobenzoyl, as discussed above.

ET Rates Predicted by Marcus Theory

A theoretical analysis provides additional support for an ET process as the mechanism of quenching of the local excited state of FA. We have modeled the rate of ET, k_{et}, derived from the TRIR measurements using the well-known semiclassical Marcus theory of ET as follows:[48–50]

$$k_{et}=\frac{2\pi H^2}{h\sqrt{4\pi\lambda(r)k_B T}}e^{-(\Delta G+\lambda(r))^2/4\lambda(r)k_B T} \quad (6)$$

$$\Delta G=-h\upsilon+(E_{ox}^{D}-E_{red}^{A})-\frac{e^2}{4\pi\varepsilon_0\varepsilon_s r} \quad (7)$$

$$\lambda(r)=\frac{e^2}{4\pi\varepsilon_0}\left(\frac{1}{\varepsilon_{op}}-\frac{1}{\varepsilon_s}\right)\left(\frac{1}{2r_A}+\frac{1}{2r_D}-\frac{1}{r}\right) \quad (8)$$

H is the electronic coupling energy of the donor and acceptor, k_B is Boltzmann's constant (J K^{-1}), T is the temperature (300 K), h is Planck's constant (6.626076×10^{-34}J s), and G is the Gibbs free energy change for the ET. The Gibbs free energy change depends on the reduction potential of the acceptor (E_{red}), the oxidation potential of the donor (E_{ox}), the electronic charge (e), the vacuum permittivity (ε_0), and the static dielectric constant of the solvent (water, $\varepsilon_s = 77.56$). The reorganization energy $\lambda(r)$ is expressed in terms of the radius of the acceptor (r_A) and donor (r_D), the distance between the donor and acceptor (r), and the optical dielectric constant ($\varepsilon_{op} = 1.33$).

We have calculated the rate of ET from PABGA to the pterin ring, using an estimate of the coupling energy between the donor and acceptor and the redox potentials of the donor (+0.93 V) and acceptor (−0.86 V). The reorganization energy is calculated using the radii of the donor and acceptor of 4 and 2.5 Å, respectively, from the energy minimized structure of FA. We estimate the coupling energy H by comparison to a series of noncovalently bonded aromatic donor–acceptor systems that are hydrogen bonded in polar and nonpolar solvents. The coupling energy for these DA pairs has been evaluated by measuring the photoinduced ET.[48] The coupling energy deduced from these experiments depends on the polarity of the solvent, increasing from 5 cm^{-1} in $CHCl_3$ to 60 cm^{-1} in toluene.[48] Using an initial estimate of 60 cm^{-1} for the 4-aminobenzoyl/pterin coupling energy, the excited-state energy of 3.06 eV, the distance r between the donor and acceptor of 5.6 Å (measured from the energy minimized structure), and the Gibbs free energy change for the ET, $\Delta G = -1.3$ eV, we calculate an ET lifetime of 16 ps at 300 K. Since the donor and acceptor of FA are covalently bonded, and since the solvent is water, a more realistic coupling energy H is 150 cm^{-1}, yielding an ET lifetime of 2.5 ps, close to the observed lifetime of 2.1 ps. The close agreement between predicted and observed ET rates provides strong support for our model of the excited-state dynamics, as summarized in Figure 8.

The other possible reaction following formation of the local pterin excited state is ET from the pterin to the 4-aminobenzoyl. We have already shown that the driving force (ΔG) is nearly identical for each of the two possible ET reactions (−1.27 eV and −1.18 eV). Since all of the other parameters of the Marcus relationship remain the same, the two possible excited-state ETs should have essentially the same rate. Therefore, both ET states will be

almost equally populated via ET reactions from the local excited state of the pterin, as shown in Figure 8. Finally, return to the ground state from each of these ET states requires the reverse ET reaction. The Marcus relation predicts that these reactions will also be very fast, and on the same order of magnitude as the forward ET reactions, because the driving forces are similar. This prediction is validated by the TRIR data. The IR transient assigned to the charge separated state (Figure 5C) shows a nearly equivalent rise of 2.0 ps and decay of 5.0 ps, reflecting the close correspondence of the formation (forward ET from local excited state) and decay (reverse ET back to ground state) rates.

ET Model

Two models have been proposed to explain excited-state ET reactions of FA, as reviewed in the Introduction, involving either intra-ET or inter-ET. Collisions between excited states of FA molecules are required for inter-ET. At the low concentrations used in our experiments, collisions of FA molecules in the short-lived singlet excited state are improbable. Such collisions are only likely for the long-lived triplet state, unless the molecules are already in contact in the GS through association of the aromatic groups. We have already demonstrated through TRIR measurements that ET from the singlet excited state is ultrafast.

(1). Concentration Dependence—If the ET reaction is between different FA molecules, this inter-ET will be concentration dependent. We have already demonstrated that the excited-state dynamics of FA are concentration dependent at low pH due to dimerization (Figure 7A). However, at low pH, no ET is observed for either the monomer or dimer. At low concentration (monomers), the singlet excited state decays by ISC to the triplet state on a time scale of hundreds of picoseconds, but no ET is observed during this time. At higher concentration (dimers), the lifetime is shortened due to stacking of the pterin rings, but again no ET is observed. By contrast, at high pH (10.0), we do observe ET for FA concentrations in the range from 5 to 60 mM. In this case, the TRIR transients are indistinguishable, as shown in Figure 7B. Since the NMR study cited previously demonstrates that dimers do not form at high pH until the concentration is much higher, the absence of a concentration dependence of the dynamics is not surprising. There is also no change in the electronic absorbance spectrum over this range, and down to much lower concentrations, which supports the conclusion that FA is monomeric over this concentration range. Taken together, the high pH results are not consistent with inter-ET, but instead support intra-ET in monomeric FA molecules.

(2). Solvent Dependence—We also investigated the solvent dependence of the ET reaction at high pH (>9.0) in mixtures of DMSO and water at a constant FA concentration of 60 mM as shown in the Supporting Information (Figure S4). The observed lifetimes for the rise and decay of the ET signatures in the TRIR spectra depend strongly on the amount of DMSO in water, ranging from 131 ps in mostly DMSO to 2 ps in pure water. Thus, the rate of ET slows with added DMSO, despite having a constant FA concentration. The rate of inter-ET should not change with constant FA concentration, again supporting intra-ET as the primary mechanism. There are two likely origins of slower intra-ET in DMSO:water mixtures. Addition of DMSO to the solution lowers the dielectric of the medium, which is predicted to slow the ET, although by less than 20% over the range studied. The second possibility is that adding DMSO perturbs the conformation of FA, leading to a change in the intra-ET rate. Support for this interpretation is found in comparison of our results with studies of intra-ET in flavin adenine dinucleotide (FAD) in DMSO:water mixtures.[51] In water, FAD has a “U” shape that brings the adenine and isoalloxazine rings close to one another. The close interaction of the two ring structures facilitates intra-ET from the adenine to the isoalloxazine. With the addition of DMSO to the solution, FAD adopts an “open” conformation that reduces the intra-ET rate, because of the increased distance between

donor and acceptor. Our results are consistent with a “U” shaped conformation of FA in water, supporting fast ET. We propose that with the addition of DMSO to the solution, FA adopts the “open” conformation, increasing the distance between the 4-aminobenzoyl and pterin structures, thus slowing the intra-ET reactions. The slower ET rate cannot be fully rationalized, however, in terms of the increased donor–acceptor distance alone. The maximum donor–acceptor distance expected for the fully open conformation is 7 Å. The ET lifetime calculated from the Marcus relationship using r = 7 Å and H = 150 cm^{-1} is 43 ps, significantly faster than what is observed for high DMSO:water ratios (131 ps for a ratio of 4:1). We have already noted that in the closed conformation there is direct overlap of the π systems for the donor and acceptor rings, which is expected to increase the coupling energy. We conclude that this π−π interaction is diminished or lost in the open conformation, reducing the coupling energy and thus further reducing the ET rate.

CONCLUSIONS

We have carried out pH-dependent, ultrafast TRIR measurements to understand the excited-state ET reactions of FA in its cationic and anionic forms. In its anionic form at pH 10.0, the TRIR spectra are consistent with fast ET between the pterin and the 4-aminobenzoyl subunits. The IR assignments are supported by analysis of the FTIR spectra of the individual subcomponents of FA, allowing separate identification of vibrational modes belonging to the pterin (PCA) and the 4-aminobenzoyl (PABGA). Thus, the transient IR spectra provide clear evidence for the excited-state transfer of an electron between the pterin and the 4-aminobenzoyl. The driving force for the ET reaction in either direction is almost identical, and therefore both reactions are nearly equally likely (Figure 8). Using Marcus theory and a reasonable estimate of the donor–acceptor coupling energy (150 cm^{-1}), we calculate an ET lifetime of 2.5 ps, in close agreement with the observed lifetime of 2.0 ps. Finally, return to the ground state from each of these ET states requires the reverse ET reaction, which happens almost as rapidly, within 5 ps. The rapid ET reactions depend on close interaction between donor and acceptor, supporting the adoption of a “U” conformation of FA in high pH solution. Upon addition of DMSO, ET becomes more unfavorable, suggesting that FA adopts a more open conformation in the mixed solvent. These data support a model in which the ET occurs directly from the π systems of the donor and acceptor rings, and not through the sigma bonds between the rings.

The cationic form of FA at low pH exhibits very different behavior. No ET is observed for this form of FA, yielding much longer lifetime of the singlet excited state. Low pH likely induces a conformational change in FA to the open form, in which the distance and coupling energy are unfavorable for ET. This conformational change causes the lowest energy absorbance in the UV–vis spectrum (a local excited state of the pterin) to shift to higher energy, consistent with the loss of the ring–ring interaction present in the closed conformation. Thus the initial singlet excited state remains localized on the pterin moiety of FA, and the excited-state charge distribution evolves with time. Furthermore, the TRIR spectra indicate that the initial excited state is localized on the pterin ring containing the carbonyl substituent, but ISC to the triplet state produces a different charge distribution, resulting in a very different transient IR spectrum. At higher concentrations (>10 mM), we observe rapid quenching of the excited state due to the formation of FA dimers having a stacking interaction between rings.

Finally, ultrafast intramolecular ET quenches the singlet excited state of FA and prevents further excited-state reactions. By contrast, conformations for which intra-ET is inhibited have more efficient ISC to the long-lived triplet state that is more likely to undergo photochemistry or to generate singlet O_2. Formation of the triplet state is crucial to the photodegradation and subsequent toxicity of FA. Therefore, conformations of FA that allow

ultrafast intra-ET and rapid quenching of the singlet excited state play a key role in preventing pathological pathways following photoexcitation of FA.

Supplementary Material

Refer to Web version on PubMed Central for supplementary material.

Acknowledgments

This work is supported by the National Institute of General Medical Sciences (P01GM068036).

REFERENCES

1. Litwack, G., editor. Folic Acid and Folates. Vol. Vol. 79. New York: Academic Press; 2008.
2. Lucock M. Mol. Genet. Metab. 2000; 71:121–138. [PubMed: 11001804]
3. Bailey, LB., editor. Folate in Health and Disease. Vol. Vol. 1. Boca Raton, FL: CRC Press; 1995.
4. Kim YI. J. Nutr. Biochem. 1999; 10:66–68. [PubMed: 15539274]
5. Kim YI. Nutr. Rev. 1999; 57:314–321. [PubMed: 10575908]
6. Joshi R, Adhikari S, Patro BS, Chattopadhyay S, Mukherjee T. Free Radical Biol. Med. 2001; 30:1390–1399. [PubMed: 11390184]
7. Hirakawa K, Suzuki H, Oikawa S, Kawanishi S. Arch. Biochem. Biophys. 2003; 410:261–268. [PubMed: 12573286]
8. Lorente C, Thomas AH. Acc. Chem. Res. 2006; 39:395–402. [PubMed: 16784217]
9. Off MK, Steindal AE, Porojnicu AC, Juzeniene A, Vorobey A, Johnsson A, Moan JJ. Photochem. Photobiol. B: Biol. 2005; 80:47–55.
10. Cabrerizo FM, Petroselli G, Lorente C, Capparelli AL, Thomas AH, Braun AM, Oliveros E. Photochem. Photobiol. 2005; 81:1234–1240. [PubMed: 16225380]
11. Tyagi A, Penzkofer A. Chem. Phys. 2010; 367:83–92.
12. Thomas AH, Lorente C, Capparelli AL, Pokhrel MR, Braun AM, Oliveros E. Photochem. Photobiol. Sci. 2002; 1:421–426. [PubMed: 12856711]
13. Martin CB, Walker D, Soniat M. J. Photochem. Photobiol. A: Chem. 2009; 208:1–6.
14. Chen X, Xu XF, Cao ZX. J. Phys. Chem. A. 2007; 111:9255–9262. [PubMed: 17629256]
15. Soniat M, Martin CB. Pteridines. 2008; 19:120–124.
16. Soniat M, Martin CB. Pteridines. 2009; 20:124–129.
17. Thiery C. Eur. J. Biochem. 1973; 37:100–108. [PubMed: 4354048]
18. Lam YF, Kotowycz G. Can. J. Chem. 1972; 50:2357–2363.
19. Getoff N. Oncol. Res. 2005; 15:295–300. [PubMed: 16408694]
20. Song QH, Hwang KC. J. Photochem. Photobiol. A: Chem. 2007; 185:51–56.
21. Thomas A, Einschlag FG, Feliz MR, Capparelli AL. J. Photochem. Photobiol. A: Chem. 1998; 116:187–190.
22. Nibbering ETJ, Fidder H, Pines E. Annu. Rev. Phys. Chem. 2005; 56:337–367. [PubMed: 15796704]
23. Stoutland PO, Dyer RB, Woodruff WH. Science. 1992; 257:1913–1917. [PubMed: 1329200]
24. Fayer, MD. Boca Raton, FL: CRC Press; 2001.
25. Rubtsov IV, Redmore NP, Hochstrasser RM, Therien MJ. J. Am. Chem. Soc. 2004; 126:2684–2685. [PubMed: 14995169]
26. Mohammed OF, Banerji N, Lang B, Nibbering ETJ, Vauthey E. J. Phys. Chem. A. 2006; 110:13676–13680. [PubMed: 17181320]
27. Weinstein JA, Grills DC, Towrie M, Matousek P, Parkerc AW, George MW. Chem. Commun. 2002:382–383.
28. Li G, Parimal K, Vyas S, Hadad CM, Flood AH, Glusac KD. J. Am. Chem. Soc. 2009; 131:11656–11657. [PubMed: 19653686]

29. Moorthy PN, Hayon EJ. Org. Chem. 1976; 41:1607–1613.
30. Swislocka R, Samsonowicz M, Regulska E, Lewandowski W. J. Mol. Struct. 2006; 792:227–238.
31. Kondo M, Nappa J, Ronayne KL, Stelling AL, Tonge PJ, Meech SR. J. Phys. Chem. B. 2006; 110:20107–20110. [PubMed: 17034182]
32. Moheno P, Pfleiderer W, DiPasquale AG, Rheingold AL, Fuchs D. Int. J. Pharm. 2008; 355:238–248. [PubMed: 18272305]
33. Zhang J, Rana S, Srivastava RS, Misra RDK. Acta Biomater. 2008; 4:40–48. [PubMed: 17681499]
34. Basyuk V, Chuiko AA. J. Appl. Spectrosc. 1990; 52:616–619.
35. Seng G, Bolard J. Biochimie. 1983; 65:169–175. [PubMed: 6405809]
36. McGovern DA, Quinn S, Doorley GW, Whelan AM, Ronayne KL, Towrie M, Parker AW, Kelly JM. Chem. Commun. 2007:5158–5160.
37. McGovern DA, Doorley GW, Whelan AM, Parker AW, Towrie M, Kelly JM, Quinn SJ. Photochem. Photobiol. Sci. 2009; 8:542–548. [PubMed: 19337669]
38. Tsuboi M, Kyogoku Y, Shimanouchi T. Biochim. Biophys. Acta. 1962; 55:1–12. [PubMed: 13922834]
39. Tripathi GNR, Su YL. J. Am. Chem. Soc. 1996; 118:2235–2244.
40. Wray WO, Aida T, Dyer RB. Appl. Phys. B: Laser Opt. 2002; 74:57–66.
41. Lian TQ, Locke B, Kholodenko Y, Hochstrasser RM. J. Phys. Chem. 1994; 98:11648–11656.
42. Oda NKT, Ichimura A. Anal. Sci. 2001; 17:i375–i378.
43. Narayanan M, Kodali G, Xing Y, Stanley RJ. J. Phys. Chem. B. 2010; 114:10573–10580. [PubMed: 20734496]
44. Kotkar RM, Srivastava AK. Sens. Actuators, B. 2006; 119:524–530.
45. Raghavan R, Dryhurst G. J. Electroanal. Chem. 1981; 129:189–212.
46. Huber R, Fiebig T, Wagenknecht A. Chem. Commun. 2003:1878–1879.
47. Poe M. J. Biol. Chem. 1973; 248:7025–7032. [PubMed: 4743511]
48. Smitha MA, Prasad E, Gopidas KR. J. Am. Chem. Soc. 2001; 123:1159–1165. [PubMed: 11456669]
49. Siders P, Marcus RA. J. Am. Chem. Soc. 1981; 103:748–752.
50. Schmidt JA, Liu J, Bolton JR, Archer MD, Gadzekpo VPY. J. Chem. Soc., Faraday Trans. 1989; 85:1027–1041.
51. Li GF, Glusac KD. J. Phys. Chem. B. 2009; 113:9059–9061. [PubMed: 19527046]

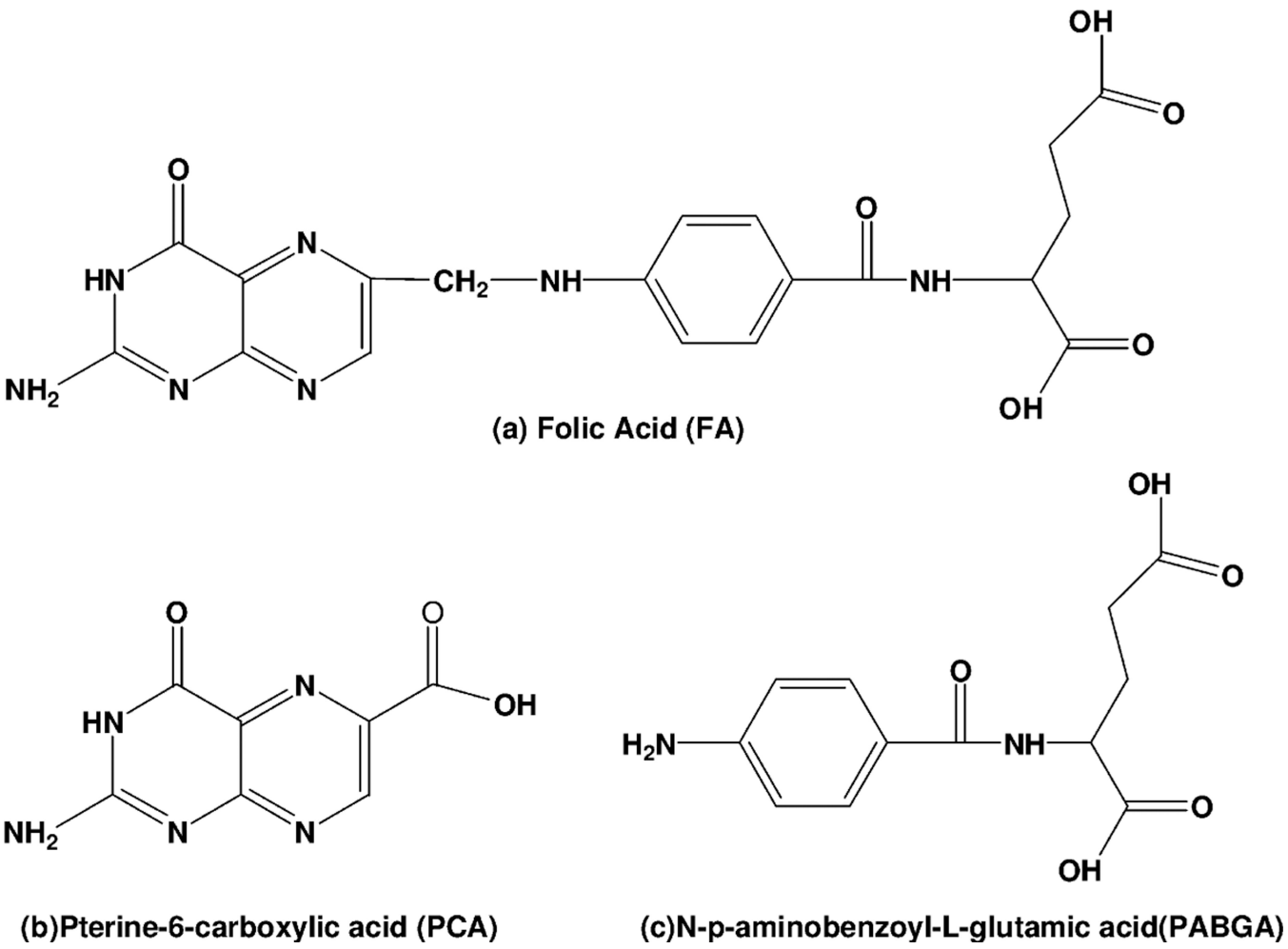

Figure 1.
Chemical structure of FA (a), PCA (b), and PABGA (c).

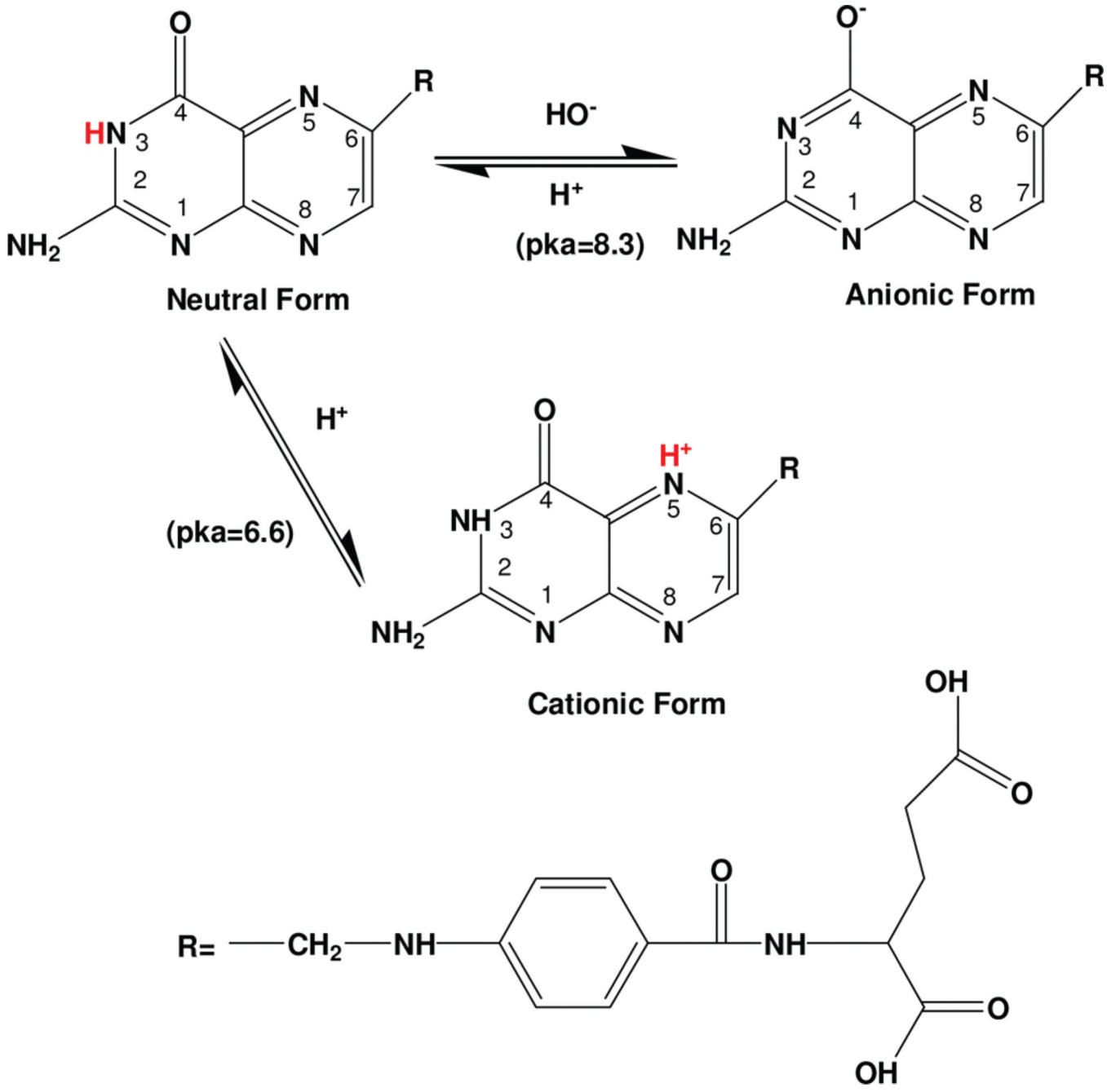

Figure 2.
Schematic for the acid–base equilibria of FA.

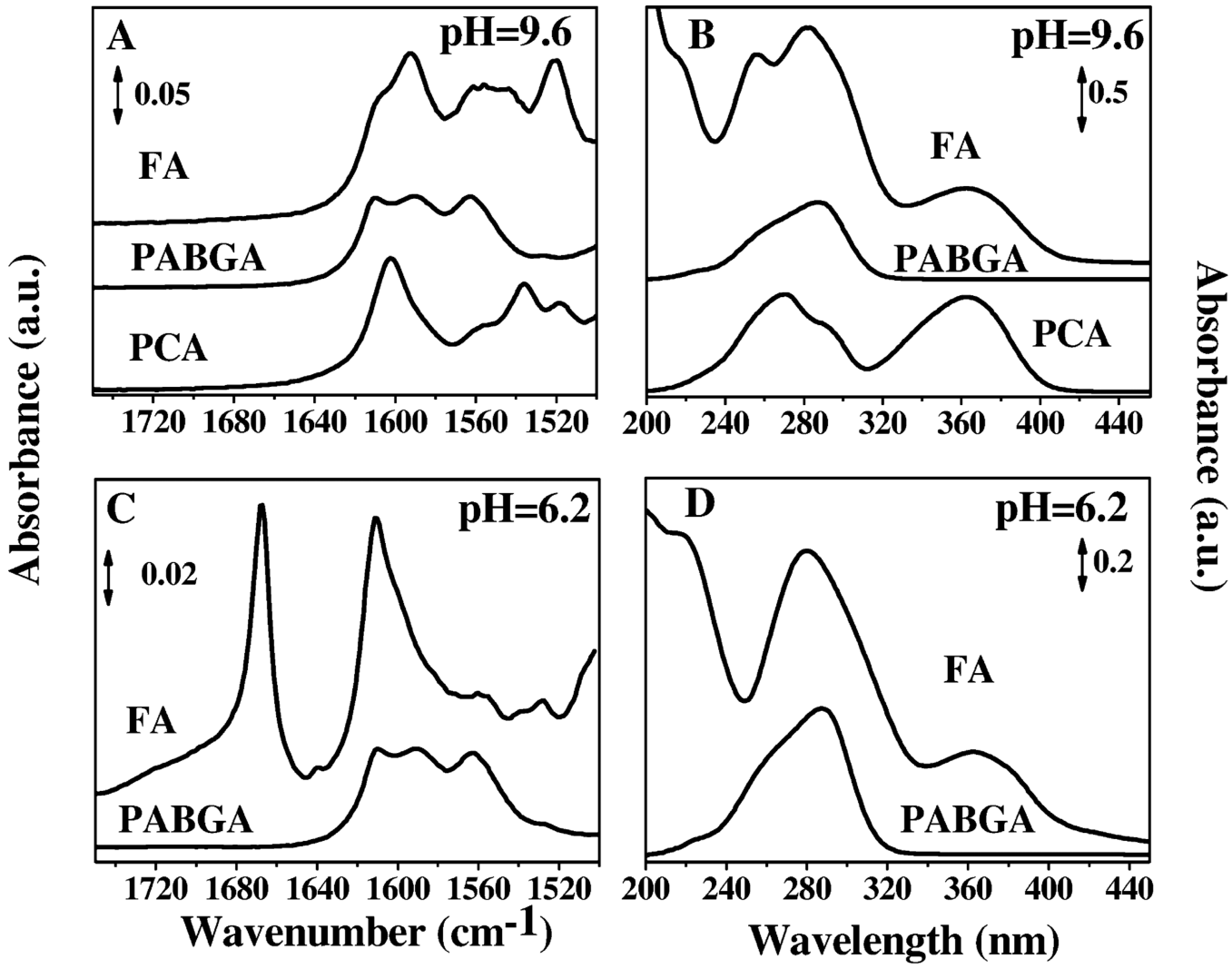

Figure 3.
FTIR (A,C) and UV–vis (B,D) absorbance spectra. Comparison of 10 mM FA, 10 mM PABGA, and 10 mM PCA at pH 9.6 (A,B) and pH 6.2 (C,D). Spectra are offset for clarity.

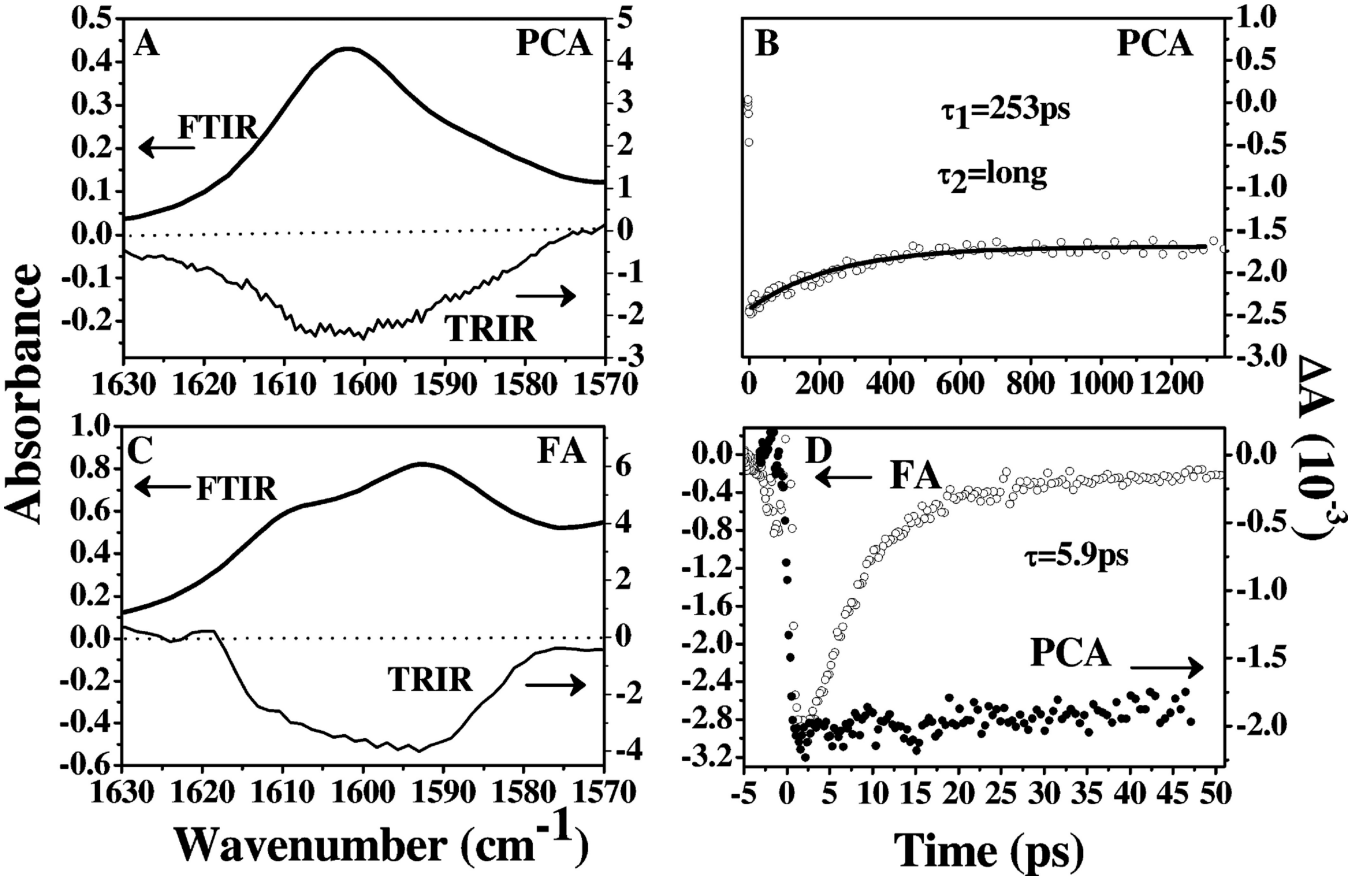

Figure 4.

Comparison of FTIR and TRIR (3 ps) of 40 mM PCA (A) and 60 mM FA (C) at pH 10; IR transient of PCA (B) and short time scale comparison (D) of IR transients of FA and PCA at 1608 cm^{-1}.

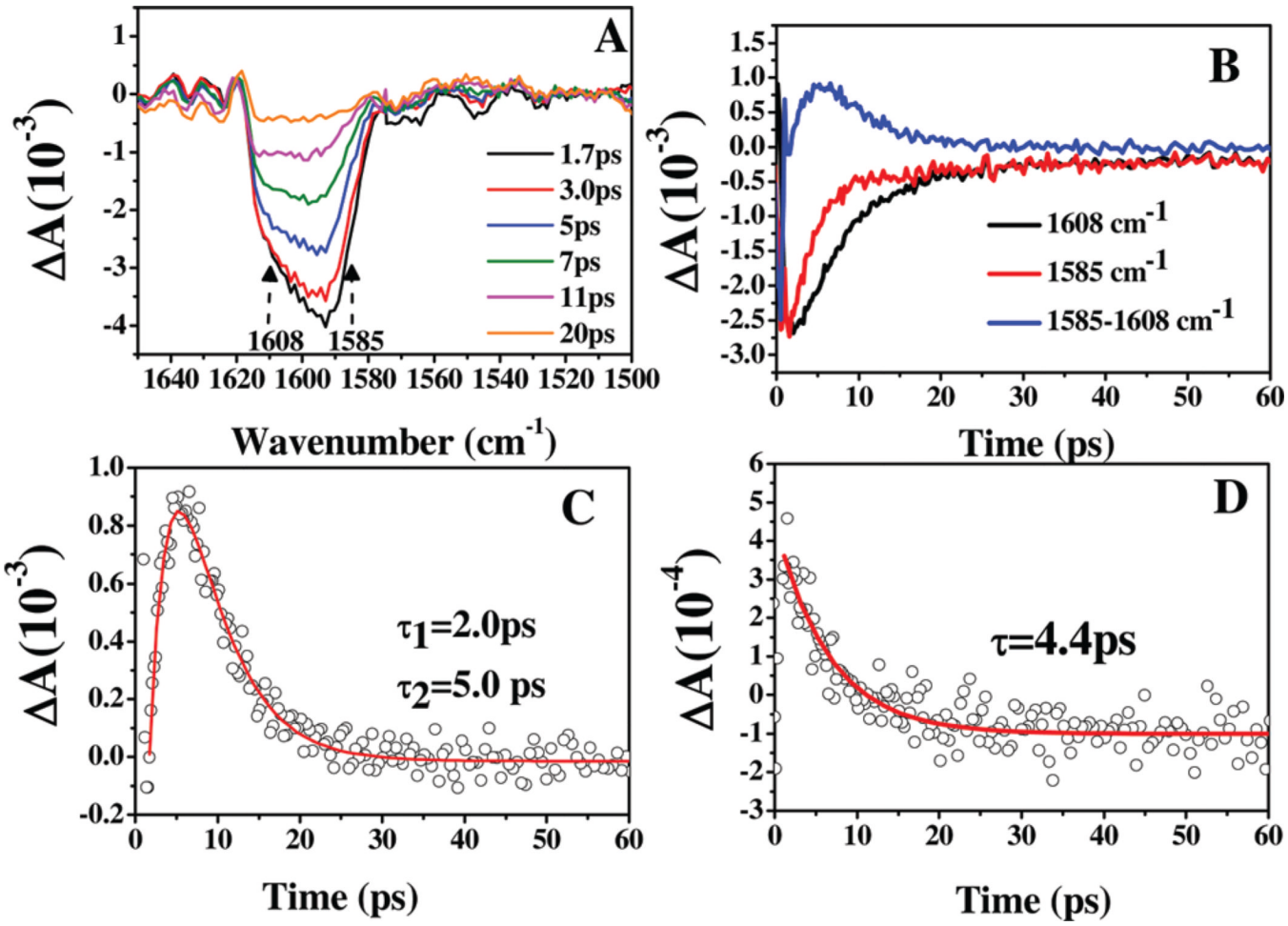

Figure 5.

FA at pH 9.6 (60 mM): (A) TRIR spectra of FA (pH 9.6) with increasing time as indicated in the figure between 1.7 and 20 ps; (B) transient IR at 1608 cm^{-1}, 1585 cm^{-1} and difference of 1585–1608 cm^{-1}; (C) double exponential fit of IR difference (1585–1608 cm^{-1}) transient; (D) single exponential fit of decay at 1630 cm^{-1}.

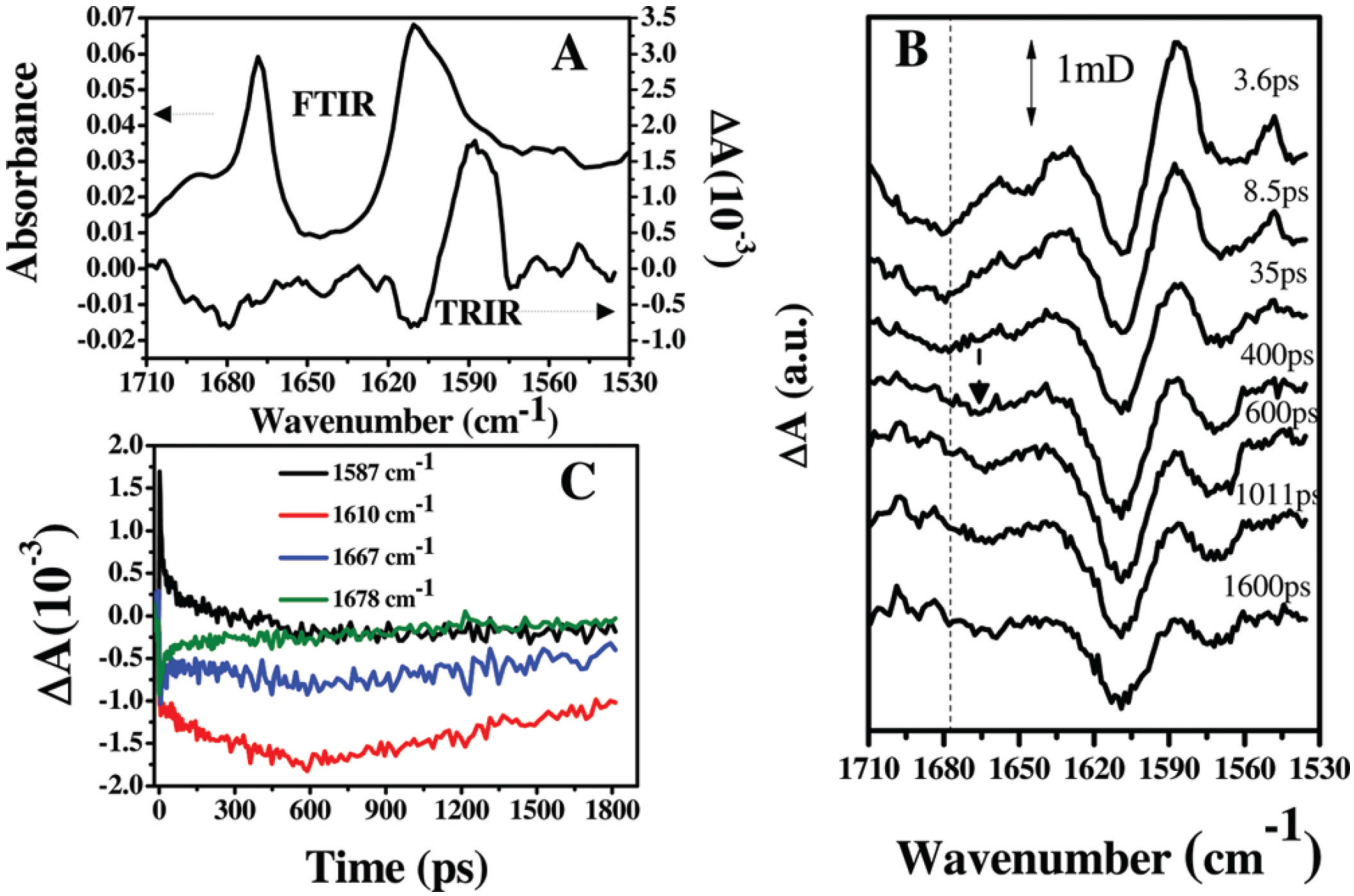

Figure 6.

FA at pH 5.8 (5 mM): (A) comparison of FTIR and TRIR spectra; (B) time evolution of the transient IR spectra; (C) selected IR transients. The IR transient at 1667 cm^{-1} has been multiplied by 2× for clarity.

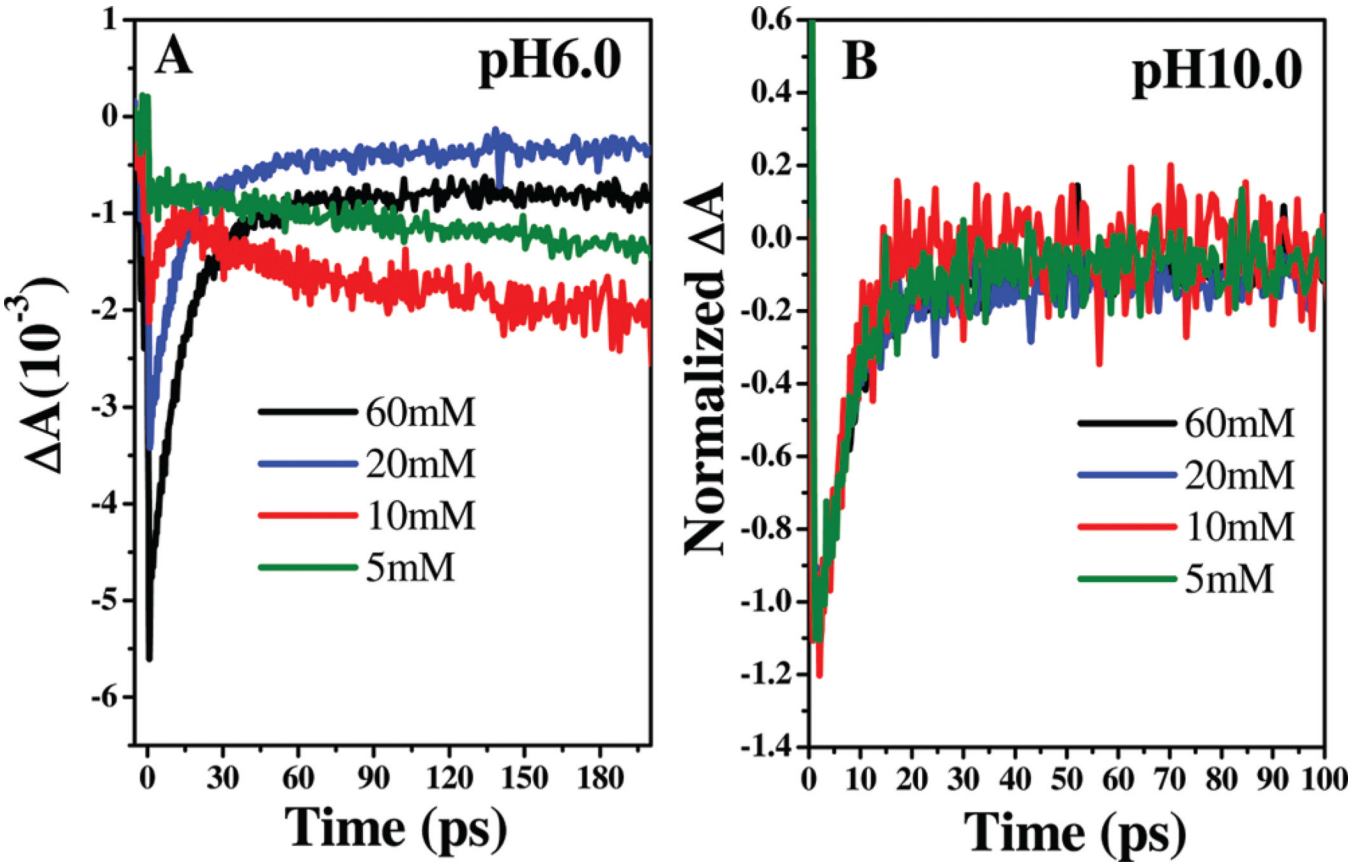

Figure 7.
Concentration dependence of IR transients obtained for FA concentrations of 5, 10, 20, and 60 mM at pH 6.0 (A) and pH 10.0 (B).

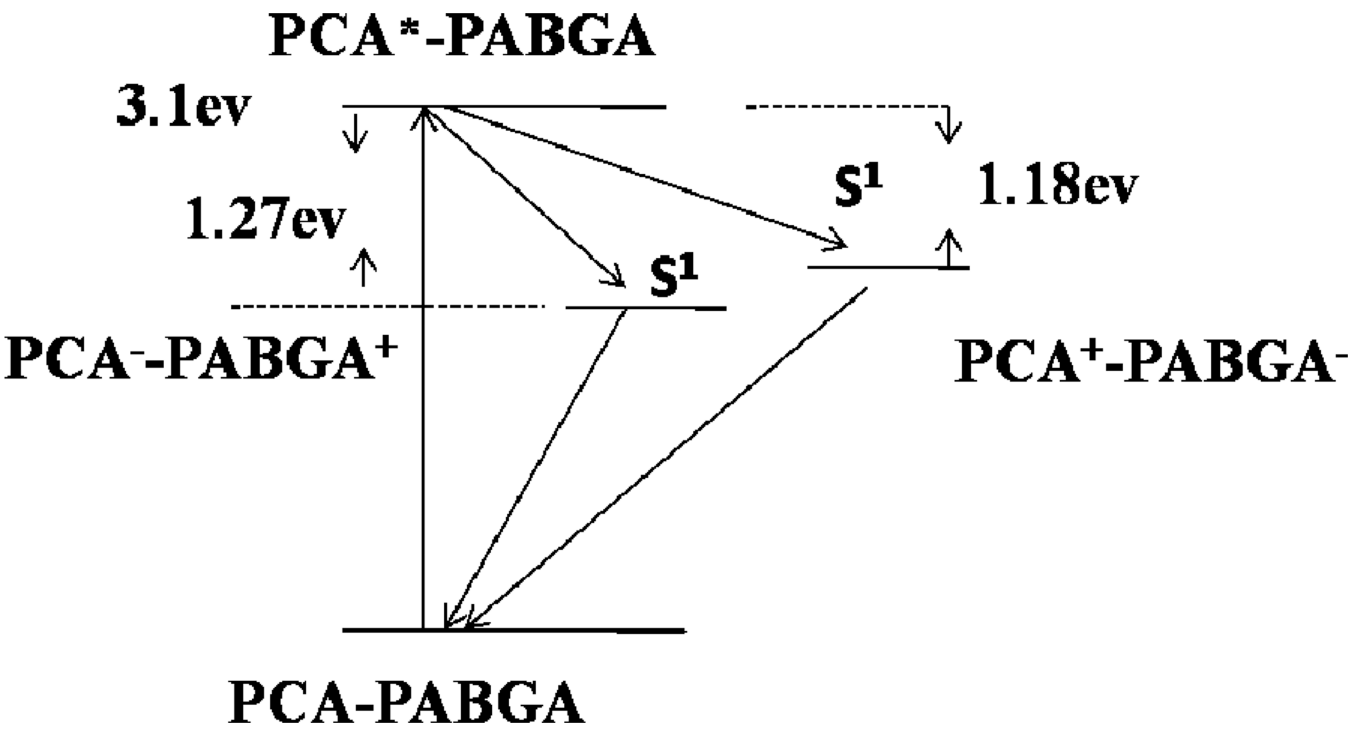

Figure 8.
Energy scheme of FA in basic solution (pH 10) excited at 400 nm.